Overdamped excitations of the free electron gas in GaN layers studied by Raman spectroscopy

M. Ramsteiner, O. Brandt, and K. H. Ploog
Paul-Drude-Institut für Festkörperelektronik, Hausvogteiplatz 5-7, D-10117 Berlin, Germany
(Received 12 December 1997)

Raman spectra of *n*-type GaN on GaAs are compared with line-shape calculations for excitations of the free electron gas. The spectral features in the frequency range of the optical phonons are well explained by plasmon-phonon scattering from an overdamped plasma system taking into account wave-vector nonconservation. The charge-density-fluctuation mechanism is found to be important for off-resonant excitation. For excitation closer to the fundamental band gap of GaN, the impurity-induced Fröhlich mechanism becomes dominant. In the latter case, the observation of a relatively narrow line at the longitudinal-optical phonon frequency is consistent with the presence of a high-density electron gas. [S0163-1829(98)01924-9]

Raman scattering by plasmon-phonon excitations has been proven to be a very useful tool for investigating free-carrier gases in doped semiconductors such as *n*-type GaAs.[1] Recently, the analysis of Raman spectra has also been applied to studying the free electron gas in *n*-type GaN.[2–7] In part of that work, the appearance of a longitudinal-optical (LO) phonon line at certain hydrostatic pressures has been interpreted as being indicative of carrier freeze-out.[2,3] However, due to the relatively short relaxation times and large effective mass associated with free electrons in GaN, the plasmon damping constant Γ is often in the range of or even larger than the plasma frequency ω_P. Raman spectra from such overdamped plasma systems cannot be treated like those from weakly damped ones with the well-known behavior of the two long-wavelength coupled plasmon-phonon modes $L^{\pm}$. In the limit of high carrier densities (n), weak damping leads to a L^- mode at the transverse optical (TO) phonon frequency (ω_{TO}) and a L^+ mode close to $\omega_P \sim \sqrt{n}$ (half width of about Γ). In contrast, from an overdamped plasma only one Raman feature in the range of the optical phonon frequencies might be observed, even in the presence of a large carrier density.[1,8,9] For example, such a spectral feature at the LO phonon frequency (ω_{LO}) was observed from *n*-type GaAs at hydrostatic pressures, where an overdamped plasma is induced by the transfer of free electrons to conduction-band minima along the Δ direction of the Brillouin zone.[10]

In the present work, we compare Raman spectra of cubic *n*-type GaN on GaAs with theoretical simulations based on the concept of overdamped plasma excitations and taking into account wave-vector nonconservation. We explain in a coherent picture the strong dependence of GaN Raman spectra on the degree of wave-vector nonconservation and the dominating scattering mechanism. Due to the similar material constants, our conclusions drawn for cubic GaN hold also for the hexagonal phase. In particular, our results might have consequences on recent work in which the appearance of a Raman feature at ω_{LO} has been discussed in terms of a free-carrier transfer into strongly localized defect states at high pressures.[2,3]

Nominally undoped GaN samples were grown by molecular-beam epitaxy on GaAs (001) substrates. The 200-nm-thick layers are predominantly cubic with a free electron density of $n \approx 1-5\times10^{18}$ cm^{-3} and mobility of $\mu \approx 50-100$ Vs/cm^2. The Raman measurements were carried out in backscattering from the epilayer surface with the sample temperature controlled by a continuous-flow cryostat. The scattered light was analyzed by a DILOR triple spectrograph equipped with a cooled charge-coupled-device array. For optical excitation, we used Ar^+ and Kr^+ ion laser lines at 2.41 and 3.00 eV, respectively. Depolarized and polarized Raman spectra were recorded in the $z(x,y)z$ and the $z(y,y)\bar{z}$ scattering configurations, where x, y, z, and $\bar{z}$ denote the [100], [010], [001], and [00$\bar{1}$] crystallographic directions of the GaAs substrate.

Typical polarized Raman spectra excited at two different photon energies are shown in Fig. 1 (dotted lines). For excitation at 2.41 eV [Fig. 1(a)], the spectrum is dominated by a broad band ranging from the TO (555 cm^{-1}) to the LO (740 cm^{-1}) phonon frequency. In addition, relatively narrow peaks at ω_{TO} and the E_2 (high) phonon frequency (569 cm^{-1}) are observed. The latter peak reflects the hex-

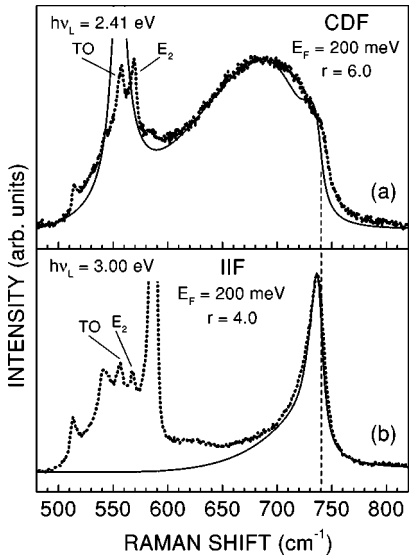

FIG. 1. Polarized Raman spectra (dotted lines) excited at 2.41 eV (a) and at 3.00 eV (b). Theoretical line shapes with a Fermi energy of 200 meV (solid lines) are shown for the CDF (a) and the IIF (b) scattering mechanisms.

agonal admixture in the dominantly cubic GaN layer. First-order scattering by TO phonons is forbidden for backscattering from a (001) surface of cubic material, but becomes allowed partly due to multiple reflections inside the transparent GaN layers.[11] The depolarized spectrum excited at 2.41 eV (not shown here) reveals a narrow LO phonon line from the depletion layers at the GaN interfaces via scattering by the deformation potential mechanism.[12] The polarized Raman spectrum excited at 3.00 eV, i.e., closer to the GaN fundamental band gap, is shown in Fig. 1(b). The contribution of second-order phonon scattering in the substrate at 540 and 590 cm^{-1} (2TO and 2LO) is now increased due to the resonance enhancement at the E_1 band gap of GaAs.[13] In contrast to the spectra excited at 2.41 eV, a relatively narrow asymmetric line close to ω_{LO} is dominating. The peak frequency, however, is about 5 cm^{-1} below that of the LO phonon line observed in the depolarized spectrum excited at 2.41 eV.[12]

The observed main features in the polarized Raman spectra cannot be attributed to scattering by lattice phonon modes of crystalline GaN. The broad structure found for excitation at 2.41 eV could be explained by disorder-activated scattering.[14] However, since our samples are *n* type, we also have to consider the contribution of plasmon-related excitations. In the presence of free carriers in heavily doped semiconductors, the LO phonons couple strongly with the collective excitations (plasmons). The carrier density dependence and the dispersion relations of the coupled modes, denoted by $L^{\pm}(q)$, are summarized in Ref. 1. For vanishing wave vectors $\vec{q}$, the frequency of the L^- mode is less than or equal to ω_{TO}, while the frequency of the L^+ mode is higher than or equal to ω_{LO}. When the plasma frequency ω_P is small (low carrier density) compared to ω_{LO}, the L^- mode has a plasmonlike character and the L^+ mode a phononlike one. In the opposite limit, L^+ is plasmonlike, while L^- shows phononlike behavior. In the latter case the L^- mode approaches ω_{TO} for vanishing wave vector ($q=0$). For a given carrier density, the L^+ mode shifts to higher frequencies with increasing wave vector $\vec{q}$ and ceases to exist (it becomes overdamped) when entering the free-particle excitation regime (Landau damping). The L^- mode also shifts to higher frequency and approaches ω_{LO} within the free-particle excitation spectrum. Consequently, wave-vector nonconservation in overdamped plasmas may lead to a broad plasmon-related band in Raman spectra covering the whole dispersion of the L^- mode between ω_{TO} and ω_{LO}. In fact, such Raman scattering features have been reported, e.g., for *p*-type GaAs layers.[1,8]

In order to simulate the Raman scattering line shapes for plasmon-related excitations, we consider the total dielectric function:

$$\epsilon(q,\omega)=\epsilon_\infty+\chi_L(\omega)+\chi(q,\omega), \tag{1}$$

where the phonon contribution of the polar lattice is given by

$$\chi_L(\omega)=\epsilon_\infty\frac{\omega_{LO}{}^2-\omega_{TO}{}^2}{\omega_{TO}{}^2-\omega^2-i\omega\gamma}. \tag{2}$$

The plasmon contribution (dielectric susceptibility of the electron gas) is calculated using the Lindhard-Mermin approach:[1]

$$\chi(q,\omega)=\frac{(1+i\Gamma/\omega)[\chi^0(q,\omega+i\Gamma)]}{1+(i\Gamma/\omega)[\chi^0(q,\omega+i\Gamma)/\chi^0(q,0)]}, \tag{3}$$

which includes the Lindhard expression for a parabolic conduction band:

$$\chi^0(q,\omega)=\frac{e^2}{2\pi^3q^2\epsilon_0}\int d^3k\ \ f(k,T)\Delta(\vec{k},\vec{q},\omega), \tag{4}$$

$$\Delta(\vec{k},\vec{q},\omega)=g(\vec{k},\vec{q},-\omega)+g(-\vec{k},\vec{q},\omega), \tag{5}$$

$$g(\vec{k},\vec{q},\omega)=\frac{1}{\hbar^2q^2/m^*+2\hbar^2\vec{q}\cdot\vec{k}/m^*+2\hbar\omega}. \tag{6}$$

Here, $f(q,T)$ is the Fermi distribution function at temperature T (we used $T=0$). An effective electron mass $m^*=0.21\,m_0$ and a damping constant $\Gamma=500$ cm^{-1} have been used for the calculations. No significant change of the line shapes was found for 100 $cm^{-1}\leq\Gamma\leq500$ cm^{-1}. Other parameters are $\omega_{TO}=555$ cm^{-1}, $\omega_{LO}=740$ cm^{-1}, $\gamma=10$ cm^{-1}, and a background dielectric constant of $e_\infty=5.25$.

For the polarized Raman spectra under investigation, we have to regard two different scattering mechanisms: The charge-density fluctuation (CDF) and the ''forbidden'' impurity-induced Fröhlich (IIF) mechanisms. The corresponding spectral line-shape functions for Raman scattering by longitudinal excitations of the coupled free-electron optical-phonon system are given by[1]

$$L(q,\omega)=q^2S(\omega)\mathrm{Im}\left\{\frac{-1}{\epsilon(q,\omega)}\right\}. \tag{7}$$

For the CDF mechanism, the factor $S(\omega)$ depends on the optical phonon frequencies and is zero at ω_{LO}. In the case of the IIF mechanism, $S(\omega)$ is a constant.[1]

The electron mobility in our *n*-type GaN samples is typically in the range of $\mu\approx100$ Vs/cm^2, which corresponds to a plasmon damping constant (collision frequency) on the order of $\Gamma=\tau^{-1}=e/\mu m^*\approx500$ cm^{-1} (τ is the collision relaxation time for free electrons). The plasma frequency for a typical carrier density of $n\approx5\times10^{18}$ cm^{-3} is also in the range of $\omega_P=\sqrt{e^2n/\epsilon_0\epsilon_\infty m^*}\approx500$ cm^{-1}. Under such conditions, an overdamped plasma system is established. In order to take into account a $\vec{q}$-nonconserving mechanism, we fold the $\vec{q}$-conserving response function $L(q,\omega)$ with a ''weight'' function $F(q)$. In the case of $\vec{q}$ nonconservation induced by impurities, this function may, to a first approximation, be taken as the square of the Fourier transform of a Yukawa-type impurity potential:[1,8]

$$F(q)=\left(\frac{4\pi}{q^2+q_{FT}^2}\right)^2, \tag{8}$$

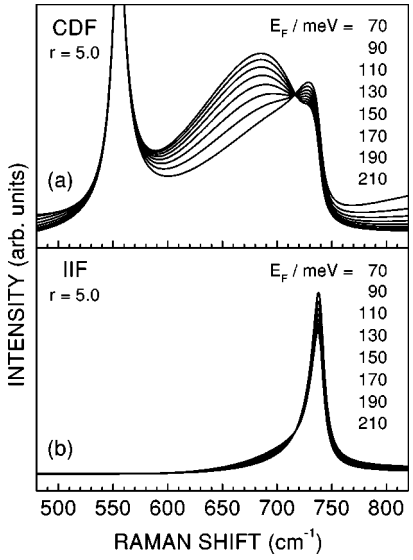

FIG. 2. Theoretical line shapes of Raman spectra for scattering by overdamped plasmon-related excitations according to the CDF (a) and the IIF (b) scattering mechanisms and different Fermi energies E_F.

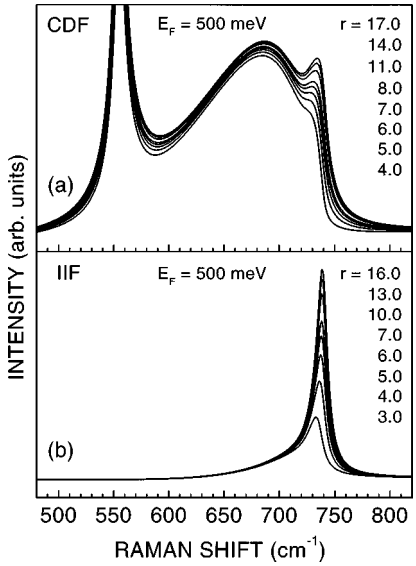

FIG. 3. Theoretical line shapes of Raman spectra for scattering by overdamped plasmon-related excitations according to the CDF (a) and the IIF (b) scattering mechanisms and different cutoff wave vectors $q_{\max}=r\ q_{\mathrm{FT}}$.

where $q_{\mathrm{FT}}=\omega_{\mathrm{P}}\sqrt{3m^*/2E_F}$ denotes the Fermi-Thomas screening wave vector. The corresponding ''weighted'' response function $I(\omega)$ averages intensities of scattering processes for q up to about q_{FT}:

$$I(\omega)=\int_0^{q_{\max}} dq\ F(q)L(q,\omega). \tag{9}$$

It should be pointed out that $I(\omega)$ converges slowly and that the line shape depends rather critically on the value $q_{\max}$ chosen as a cutoff. This cutoff is taken to qualitatively correspond to the decrease in the electron-phonon coupling with increasing q.[1]

Line shapes obtained from Eqs. (1)–(9) are shown in Fig. 2 for Fermi energies (E_{F}) ranging from 70 to 210 meV ($n=8\times10^{18}-4\times10^{19}$ cm^{-3}) and a cutoff wave vector $q_{\max}=5.0\,q_{\mathrm{FT}}$. The calculated spectra according to the CDF mechanism [Fig. 2(a)] are quite similar to the measured spectra excited at 2.41 eV. For increasing Fermi energy, a maximum at about 685 cm^{-1} evolves, and the calculated line shapes agree very well with the experimental one. [The pronounced structure at ω_{TO} is an artifact due to the prefactor $S(\omega)$ in Eq. (7).] The theoretical spectra for the IIF mechanism [Fig. 2(b)] closely resemble the spectra measured for excitation at 3.00 eV with a relatively weak dependence on E_{F}. The peak height decreases, and the asymmetry becomes more pronounced with increasing E_{F}. As shown in Fig. 1 (solid lines), the best agreement for both excitation lines (scattering mechanisms) is obtained using a Fermi energy of about 200 meV.

The influence of the cutoff wave vector $q_{\max}$ on the calculated line shapes is illustrated in Fig. 3 for a Fermi energy of 200 meV. The cutoff wave vector is given in units of the Fermi-Thomas screening wave vector: $r=q_{\max}/q_{\mathrm{FT}}$. In the line shape according to the CDF mechanism [Fig. 3(a)], a pronounced structure at ω_{LO} evolves with increasing $q_{\max}$. This behavior is explained by the dispersion of the L^- maximum in $L(q,\omega)$, which approaches ω_{LO} for large q values.[1] The line shape of the IIF mechanism [Fig. 3(b)] reveals only a weak dependence on $q_{\max}$. Oppositely to the dependence on E_{F}, the peak height increases and the asymmetry becomes less pronounced with increasing $q_{\max}$. The best agreement for both scattering mechanisms (excitation lines) is found for $r\approx5.0$. In Fig. 1 the theoretical line shapes for the CDF and IIF mechanisms (solid lines) are compared with the corresponding measured spectra using $r=6.0$ and $r=4.0$, respectively.

The Fermi energy of 200 meV used for the calculated line shapes in Fig. 1 corresponds to a carrier density of $n=4\times10^{19}$ cm^{-3}, which is much higher than those measured. The Fermi energy enters in our calculation mainly via the Thomas-Fermi vector q_{FT} in the function $F(q)$, which describes the wave-vector nonconservation. The particular expression used for $F(q)$ in Eq. (8) implies, however, that only the ionized donors, which contribute to the free electron gas, are responsible for wave-vector nonconservation. This assumption leads certainly to a considerable overestimation of the Fermi energy and, therefore, the carrier density in our samples. In addition, photocurrent measurements on intentionally compensated GaN/GaAs samples indicate that the carrier density can be increased considerably by the below-band-gap excitation used for our Raman measurements.

The measured Raman spectra are well described by plasmon-related excitations assuming that the CDF mechanism dominates for excitation at 2.41 eV and the IIF mechanism for excitation at 3.00 eV. In fact, it is expected that the IIF mechanism becomes more important, when approaching the resonance condition with the GaN fundamental band-gap energy of 3.3 eV.[11,15] In our calculations, we presume that scattering occurs by the CDF and the IIF mechanism alone for excitation at 2.41 and 3.00 eV, respectively. In general, scattering by both of these mechanisms will occur in parallel. The Raman features discussed here are not observed for highly resistive, comparatively pure GaN/GaAs samples sup-

porting our assignment to excitations of the free electron gas. It should be emphasized that in the framework of our work, a comparatively narrow line at the LO phonon frequency [see Fig. 1(b)] may be observed even in the presence of a high-density free electron gas ($n \sim 10^{19}$ cm^{-3}).

In summary, we explain Raman scattering features of n-type GaN layers on GaAs by overdamped excitations from the free electron gas. Assuming wave-vector nonconservation, the spectral structures in the range of the optical phonons are explained by the contribution of the charge-density fluctuation and the impurity-induced Fröhlich mechanisms. The latter mechanism becomes dominant for excitation relatively close to the resonance with the fundamental band gap of GaN. Our finding, that under certain conditions a Raman feature at the LO phonon frequency may be observed also at large carrier densities, should be considered for the interpretation of recent work on localized defect states.[2,3]

We would like to thank H. Yang for sample growth, L. Schrottke for photocurrent measurements, and the German Ministry of Education and Research (BMBF) for financial support of part of this work.

[1] For a review see, e.g., G. Abstreiter, M. Cardona, and A. Pinczuk, in *Light Scattering in Solids IV*, edited by M. Cardona and G. Güntherodt (Springer, Berlin, 1984), p. 5, and references therein.
[2] P. Perlin, T. Suski, H. Teisseyre, M. Leszczynski, I. Grzegory, J. Jun, S. Porowski, P. Boguslawski, J. Bernholc, J. C. Chervin, A. Polian, and T. D. Moustakas, Phys. Rev. Lett. **75**, 296 (1995).
[3] C. Wetzel, T. Suski, J. W. Ager III, E. R. Weber, E. E. Haller, S. Fischer, B. K. Meyer, R. J. Molnar, and P. Perlin, Phys. Rev. Lett. **78**, 3923 (1997).
[4] T. Kozawa, T. Kachi, Y. Taga, and M. Hashimoto, J. Appl. Phys. **75**, 1098 (1994).
[5] D. Kirillov, H. Lee, and J. S. Harris, Jr., J. Appl. Phys. **80**, 4058 (1996).
[6] F. Demangeot, J. Frandon, M. A. Renucci, C. Meny, O. Briot, and R. L. Aulombard, J. Appl. Phys. **82**, 1305 (1997).
[7] H. Siegle, A. Hoffmann, L. Eckey, C. Thomsen, J. Christen, F. Bertram, D. Schmidt, D. Rudloff, and K. Hiramatsu, Appl. Phys. Lett. **71**, 2490 (1997).
[8] D. Olego and M. Cardona, Solid State Commun. **32**, 375 (1979).
[9] G. Irmer, V. V. Toporov, B. H. Bairamov, and J. Monecke, Phys. Status Solidi B **119**, 595 (1983).
[10] A. Pinczuk, S. G. Louie, B. Welber, J. C. Tsang, and J. A. Bradley, in *Physics of Semiconductors 1978*, edited by B. L. H. Wilson (Institute of Physics, London, 1979), p. 1191.
[11] M. Cardona, in *Light Scattering in Solids II*, edited by M. Cardona and G. Güntherodt (Springer, Berlin, 1982), p. 153.
[12] M. Giehler, M. Ramsteiner, O. Brandt, H. Yang, and K. H. Ploog, Appl. Phys. Lett. **67**, 733 (1995).
[13] R. Trommer and M. Cardona, Phys. Rev. B **17**, 1865 (1978).
[14] M. H. Brodsky, in *Light Scattering in Solids I*, edited by M. Cardona (Springer, Berlin, 1975), p. 205.
[15] D. Behr, R. Niebuhr, J. Wagner, K.-H. Bachem, and U. Kaufmann, Appl. Phys. Lett. **70**, 363 (1997).